STUDY OF RIVER BED BEHAVIOR AT INTAKES AND OUTLETS OF TALKHA THERMAL POWER PLANT

Kassem Salah El-Alfy

Irrigation & Hydraulics Dept., Faculty of Eng., Mansoura University, Egypt

ABSTRACT

In this research paper the analytical solution for the problem of the channel junction with combining flow was applied on the outlets of Talkha thermal power plant and compared with the field investigation. Also, the field data were presented to be used in describing the general flow features and bed characteristics at both distributing and combining types of channel junctions at Talkha thermal power plant on Damietta Nile branch. It was found that the analytical solution for the problem of the channel junction with the combining flow was approximately consistent with the field investigation. Also, the study showed that both the junction angle and the discharge ratio had an effective influence on the free streamline position. The studying of the bed profile showed that a sedimentation zone was occurred downstream the outlets accompanied with the flow separation zone at the channel junction. Also, the deposition occurs upstream the distributing junction due to the effect of the transverse flow towards the intakes. The measurements of the cross-sections indicated that the formation of the deposition zone in the left side of the stream results in a scour at the right side of the stream. The analysis of the field data showed that the maximum flow depth is directly proportional to the sedimentation width. Also, the relatively smooth slope angle of the combining channel decreases the effect of the tributary flow on the scour in stream bed in the downstream.

Keywords: Junction – Sedimentation – Separation zone – Free stream line – Stagnation point.

INTRODUCTION

The flow at channel junctions was firstly studied by Taylor [13]. He studied the effect ratio of two channels on flow characteristics. Webber and Greated [14] studied the general flow characteristics at channel junction. In 1979 Lin and Soong [8] studied the energy loss through the junction. Pashupati et al. [9] used the conformal mapping to approximate the flow pattern in channel junction. Best and Reid [1] studied the separation zone physically. In 1988 Ramamurthy et al. [10] reported extensive studies and methods for prediction of the flow depth increase at the channel junction. Also, the open channel junction problem was studied by Biron et al. [2], Hsu et al. [4], Joy et al. [5], and Larry et al. [7]. Based on applying the momentum principle on the control volumes at the junction, Shazy et al. [12] developed a one dimension theoretical model for subcritical flows in combining open channel junction.

THEORETICAL APPROACH

Stagnation Point

The stagnation point could be calculated according to Pashupati et al. [9] by using the conformal mapping theorem as follows:

$$b_1 = k_1 \pi \frac{a^{(1-\alpha/\pi)}}{(1+a)(b-a)} \tag{1}$$

$$b_2 = \frac{k_1 \pi}{(1+a)(1+b)} \tag{2}$$

$$b_3 = k_1 \pi \frac{b^{(1-\alpha/\pi)}}{(1+b)(b-a)} \tag{3}$$

in which

b_1, b_2, b_3	the widths of first, second, and third channels at the junction;
K_1, a, b	constants; and
α	junction angle.

Dividing Eqs. 2 and 3 by Eq. 1 yields:

$$\frac{b_2}{b_1} = \frac{(b-a)}{(1+b)a^{(1-\alpha/\pi)}} \tag{4}$$

$$\frac{b_3}{b_1} = \frac{b^{1-\alpha/\pi}}{a^{1-\alpha/\pi}} \frac{(1+a)}{(1+b)} \tag{5}$$

Eqs. 4 and 5 could be solved together to calculate the constants *a* and *b* for the known values of b_1, b_2, b_3, and α. In conformal mapping the channel junction could be treated as a source and a sink. As illustrated in Fig. 1, the branches 1 and 2 are treated as sources, while branch 3 is treated as a sink. The strength of two sources are v_1b_1/π, v_2b_2/π, while the strength of the sink is $(v_1b_1 + v_2b_2)/\pi$.

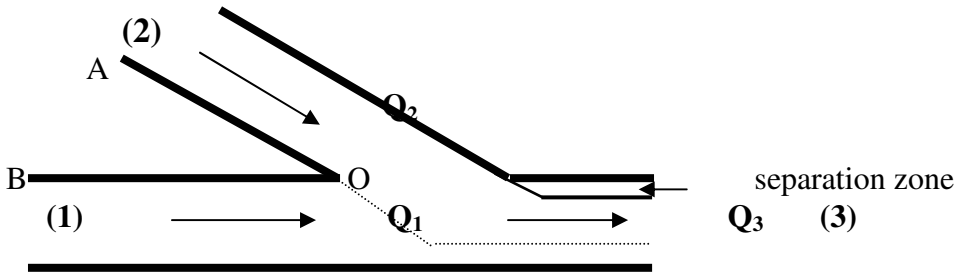

Fig. 1 Layout of a combining channel junction

Using the complex potential in ξ-plan as follows:

$$\omega = \frac{V_1 b_1 + V_2 b_2}{\pi} \ln(\xi - b) - \frac{V_1 b_1}{\pi} \ln(\xi - a) - \frac{V_2 b_2}{\pi} \ln(\xi + 1) \qquad (6)$$

in which

ω	complex variable representing rectangular flow field = φ +iψ;
V_1, V_2	mean velocities at branches 1 and 2, respectively;
a,b	constants; and
b_1, b_2	widths of branches 1 and 2, respectively.

Differentiating Eq. 6 yields:

$$\frac{d\omega}{d\xi} = \frac{V_1 b_1 + V_2 b_2}{\pi} \frac{1}{\xi - b} - \frac{V_1 b_1}{\pi} \frac{1}{\xi - a} - \frac{V_2 b_2}{\pi} \frac{1}{(\xi + 1)}$$

The velocity at any point can be obtained as follows:

$$-\frac{d\omega}{dZ} = -\left(\frac{d\omega}{d\xi}\frac{d\xi}{dZ}\right) = (-V_x + iV_y) = \frac{V_1 b_1}{\pi} \frac{(\xi+1)(\xi-b)}{K\xi^{(1-\alpha/\pi)}} + \frac{V_2 b_2}{\pi} \frac{(\xi-a)(\xi-b)}{K\xi^{(1-\alpha/\pi)}} - \frac{V_1 b_1 + V_2 b_2}{\pi} \frac{(\xi+1)(\xi-a)}{K\xi^{(1-\alpha/\pi)}} \qquad (7)$$

in which

V_x, V_y are velocity components in X and Y directions, and dz/dζ is an expression for the transformation function.

$$\frac{dz}{d\zeta} = \frac{k\zeta^{(1-a/\pi)}}{(\zeta+1)(\zeta-a)(\zeta-b)}$$

The stagnation point is a point located on the boundary AOB as illustrated in Fig.1, in which the free streamline $\psi = V_1 b_1$ intersect the boundary at the stagnation point. At the stagnation point the flow velocity equals zero i.e. (-dω/dZ)=0, then Eq. 7 equals to zero.

$$\frac{V_1 b_1}{\pi} \frac{(\xi+1)(\xi-b)}{K\xi^{(1-\alpha/\pi)}} + \frac{V_2 b_2}{\pi} \frac{(\xi-a)(\xi-b)}{K\xi^{(1-\alpha/\pi)}} - \frac{V_1 b_1 + V_2 b_2}{\pi} \frac{(\xi+1)(\xi-a)}{K\xi^{(1-\alpha/\pi)}} = 0$$

or

$$\xi = \frac{V_2 b_2 a(1+b) - V_1 b_1 (b-a)}{V_1 b_1 (b-a) + V_2 b_2 (1+b)} \qquad (8)$$

The discharge ratio $n_q = V_2 b_2/(V_1 b_1 + V_2 b_2)$ (9)

Substitution of Eq. 9 into Eq. 8 yields:

$$\xi = \frac{n_q b(1+a) - (b-a)}{n_q(1+a) + (b-a)} \qquad (10)$$

Pashupati et al. [9] stated that for any value of the channel junction angle (α), the position of the stagnation point locates along the boundary AOB depending on the value of n_q. They stated that the stagnation point lies on boundary AO for the values of ξ=-1to 0, while it lies on boundary OB for ξ=0 to a. Also, the stagnation point coincide with corner O when ξ=0 at critical value of discharge ratio n_{qcr} = (b-a)/b(1+a).

The Free Stream Line

The flow of water past a corner has to be separated from the boundary at this corner, in which a free streamline is formed. The free streamline could be defined as the streamline that separate the flow in motion from the flow in rest. Also, both the velocity and pressure remain constant along the free streamline. Pashupati et al. [9] concluded that when the stagnation point lies on the main channel boundary the coordinates of the free streamline function could be treated as follows:

$$\frac{x}{b_3} = -\frac{2}{\pi}\int_0^{\varphi} \cos f \tan\varphi d\varphi \qquad \frac{y}{b_3} = 1 - \frac{2}{\pi}\int_0^{\varphi} \sin f \tan\varphi d\varphi$$

in which f, φ, and ξ are auxiliary variables, and b_3 is the width of the main channel.
The results of Pashupati et al. [9] were used in derivation formulas describing the free streamline, which were used in this study. They [9] stated that the maximum width of the free stream line at the channel junctions ranged among 0.257, 0.537, and 0.763 of the main channel width for the tributary channel connection angles of 30^0, 60^0, and 90^0, respectively, provided that the stagnation point lies on the boundary of main channel. But when the stagnation point lies on the boundary of the tributary channel they stated that the aforementioned values were 0.1995, 0.341, and 0.471.

The Settling Process

The settling process of the suspended sediment is controlled by both drag force affecting particles and fall velocity of particles. The unit tractive force due to flow on the channel bed is $\tau_b = \gamma RS$.

in which
τ_b shear stress on bed;
γ specific weight of the flow;
R hydraulic radius; and
S longitudinal slope of water surface.

The critical shear stress at which the top layer is about to move τ_{cr} could be computed as $\tau_{cr} = C_f\, d(\gamma_s - \gamma)$

in which
γ_s specific weight of bed particles;
C_f constant; and
d grain diameter = d_{50} for nonuniform bed material.

According to Kalinske [6] C_f =0.12, then
τ_{cr}= 0.12 (γ_s- γ) d_{50}

As stated by Ruby [11], the fall velocity could be computed according to the following formula:

$$W = F[D_s g(\rho_s - \rho)/\rho]^{1/2} \quad (11)$$

in which

W fall velocity;
D_s particle diameter;
ρ_s sediment density;
ρ fluid density;
F constant = 0.79;
γ_s specific weight of sediment;
ν kinematic viscosity (10^{-6} m^2/s); and
γ specific weight of water.

FIELD INVESTIGATION

The cooling system of Talkha thermal power plant, which lies on the left bank of Damietta Nile branch at km (144.200) consists of two intakes and two outlets. The first intake for 2x50 MW units consists of three vents of width 3.65 m and separated by two piers of 0.75 m width, while the second intake of 2x210 MW units consists of two vents of 11.00 m with a pier of width 1.0 apart. The distance between the two intakes is approximately 41.50 m. The outlets are in the downstream of the intakes by approximately 220 m. The first outlet is for 2x210 MW units, while the second one is for 2x50 MW units. The general layout of the cooling system is illustrated in Fig. 2. The discharge used for the cooling system is 2.11 million cubic meters per day, which is considered 46.88% of the minimum flow of the Nile branch, 10.6% of the maximum discharge, 33% at measuring time, and 60 % of the flow discharge at winter mentaince period [3].

The surveying of the bed characteristics was carried out by using global positioning system (GPS) and echo sounder, which covers about 600 m upstream the intakes and 600 m downstream the outlets as illustrated through some selected cross-sections, Fig. 3. The flow velocities were also measured along the transverse direction of the cross-sections at four positions as illustrated in Fig. 4. At each point, the velocity was measured at depths 0.2d, 0.6d, and 0.8d by using current meters. At each depth the reading of the current meter was repeated three times and the average value at each point was calculated. The water surface slope at power plant site was also measured, which was found to be 1.4 cm/km. Also, a bed sample was taken to find the different properties of the bed particles.

The survey of the bed indicated that sedimentation occurs in the upstream of the intake in left side of the stream between the level (0.50) to (1.50) with a length of about 600 and maximum width of 71 m. Also, the sedimentation between the levels (0.50) and (1.50) occurs downstream the outlets with a length of about 536 m with maximum width of 98.0 m. On the contrary it is found that scour occurs at the right bank in opposite side of sedimentation zone, in which the bed level was (–7.50) at the cross-section of maximum sedimentation width upstream the intakes. The sedimentation upstream the intake and downstream the outlet of the power plant is shown in Fig. 5.

NUMERICAL INVESTIGATION

1- Upstream the intakes

The measured values of both flow and sediment properties at a normal cross-section in the downstream of Talkha thermal power plant on Damietta Nile branch were as follows:

d_{50}=0.32 mm, γ_s=2.65, γ_s^- =1.65, $\nu = 10^{-6}$ m^2/s, δ_L=0.102 t sec^2/m^4, δ_p=0.180 t.sec^2/m^4, and $\mu = 11.42 \times 10^{-5}$ kg sec/m^2.

The cross-section properties were; A= 424.5 m^2, P=205 m, R= 2.07 m, while at the cross-section at maximum sedimentation width upstream the intakes was; A= 343 m^2, P=197 m, and S= 1.4 cm/km

The shear stress affected bed (τ_b) = γRS

At the cross-section of maximum sedimentation width; R=343/197 =1.74, S= 1.4 cm/km, then

$\tau_b = 1*1.74*1.4 *10^{-5} = 2.436 *10^{-5}$ t/m^2

The critical shear affecting bed $\tau_{cr} = 0.12 (\gamma_s - \gamma) d_{50}$

$\tau_{cr} = 0.12 (2.68-1) 0.32 *10^{-3} = 6.45*10^{-5}$

As $\tau_b < \tau_c$ then, there is no motion for the bed particles at this section.

The fall velocity of the suspended particles could be computed according to Eq. (11).

$$w = F\,[D_s g(\rho_s - \rho)/\rho]^{1/2}$$

$$w = 0.79[0.32x10^{-3}x9.81(0.18-0.102)/0.102]^{1/2}$$

The fall velocity (ω) = 3.9 cm/s

The longitudinal velocity at the section of maximum sedimentation width upstream the intakes beside the left bank was found to be less the fall velocity through the transverse distance up to 65 m width from the left bank as illustrated in Fig. 4-A.

2- Downstream the outlets

Determination of stagnation point and free streamline for the compound outlet

Junction properties: b_1= 201 m, b_2= 63.0 m, and b_3= 211 m.

α (mean) = (60°+38°)/2 = 49°

$n_q = Q_2/Q_3$= 24.44/72.38 = 0.33

From Pashupati et al. [9] it is found that the values of both a and b are approximately 1.1325 and 3.669, respectively.

$$\xi = \frac{n_q b(1+a)-(b-a)}{n_q(1+a)+(b-a)}$$

Since the value of ξ is very near to zero, the stagnation point could be considered at the corner point O as illustrated in Fig. 1 [9].

$$\xi = \frac{0.33*3.669(1+1.1325)-(3.669-1.1325)}{0.33(1+1.1325)+(3.669-1.1325)} = 0.014$$

The derived formula describing the free streamline was applied on the two outlets of Talkha power station as illustrated in Fig. [6].

ANALYSIS AND DISCUSSION OF THE RESULTS

The cross-sections profiles of Damietta Nile branch at Talkha thermal power plant site are shown in Fig. 3. Figs. 3-a to 3-c show the cross-sections in the upstream of the intakes, Fig. 3-D shows the cross-section between the intake and the outlet, and Figs. 3-E to 3-G illustrate the cross-sections downstream of the outlets. The longitudinal profile of the river in site of the power plant shows that the dead zone of the flow starts at 15 m upstream the intake and extends to more than 600 in the upstream as shown in Fig. 5. Also, a sedimentation zone between levels (0.50) to (1.50) was formed in accompanying to the separation zone downstream the outlet of the power plant as shown in Fig. 5.

The sedimentation occurs upstream the intake of 2x210 MW units at the left side of the river could be explained due to the fact that the average fall velocity of the suspended sediment was more than the average longitudinal velocity at the left bank as previously illustrated. Also, this could be referred to the shear stress affecting bed in this zone is smaller than the critical shear stress as calculated before due to small values of flow depth. As the flow velocity besides the left bank is approximately equal to zero, then the suspended load is settled. Also, the formation of the dead zone upstream the intake is referred to the transverse flow towards the intakes, which make an angle 90^0 with the flow direction. The transverse flow towards the intakes works as an immersed weir. The existence of this imaginary immersed weir causes both the suspended and bed load resulted from the cross-current due to the existence of the power plant reach in the inner bank of a bend of the stream to be settled due to the high fall velocity compared with the longitudinal velocity at the left bank upstream the intakes. Also, the measurements of the cross-sections indicated that the formation of the sedimentation zone in the left side of the stream decrease the area of the cross-section, which causes the velocity to be increased in the right side of the stream, which causes scour and hence the flow depth increases as shown in Fig. 3-B.

Fig. 6 shows that the free streamline at the outlet of 2x210 MW units is dominated the free streamline at the outlet of 2x50 MW units. This could be attributed due to the fact that the formula controlling the free streamline depends mainly on the junction angle (α), and the discharge ratio (n_q). For the outlet of 2x210 MW, it is found that both the junction angle (α), and the discharge ratio (n_q) are bigger than those the corresponding in 2x50 MW. This means that the coordinates in y-direction of the free streamline resulted from 2x210 MW units are bigger than theses for the free streamline resulted from 2x50 MW units. Fig. 7 illustrates the free streamline that represents the two-combined outlets. It is obvious that the free streamline is very similar to the free streamline of 2x210 MW units. This could be explained due to the fact that the values of junction angle (α), and the discharge ratio (n_q) of the outlet of 2x210 MW units are bigger than those the corresponding values in 2x50 MW units. The water body between the free-streamline and the left bank of the stream was approximately in stagnation status. The separation zone could be attributed due to the effect of the momentum of tributary channel, which causes the flow in the main channel to be separated at the downstream of the junction.

Fig (8) shows the relationship between the dimensionless sedimentation zone width versus the corresponding dimensionless flow depth. It is found that the maximum flow depth is directly proportional to the sedimentation width. This could be explained due to the existence of the power plant in the inner curve of a bend. Also, as the passing discharge in the river branch is constant and the cross-sectional area is decreased, then the depth of the flow is naturally increased to adjust the river regime.

The cross-section of the river between the intake and the outlet shows that the maximum depth was smaller than the flow depth in upstream the intakes as illustrated in Fig. 3-E. This could be explained due to the fact that the discharge between the intake and the outlet is smaller than the normal discharge in both the upstream and the downstream of the power plant position by 24.44 m^3/s. The small discharge means that the longitudinal flow velocity is very small compared with the falling velocity, which results in settling both the bed load and suspended load resulted from scour at the outer bank of the bend.

From the bed profile at the outlet, it was found that the maximum flow depth occurs in the opposite direction of the outlet i.e. at the right bank as shown in Fig. 3-F. This could be attributed due to the effect of the separation zone, which directed the flow towards the right bank of the stream. Fig. 10 shows a comparison between the relationships of the maximum flow depth versus the sedimentation widths at both the intakes and the outlets. The figure shows that for the same sedimentation width, the maximum flow depth in upstream the intake is bigger than that occurs downstream the outlet This could be explained due to the fact that the width of the stream upstream the intakes is smaller than the width of the stream in downstream of the outlet, beside that the curvature of the stream upstream the intake is bigger than that existed downstream the outlet Also, the relatively smooth angle of slope of the outlet flow decreases the effect of the tributary flow on the scour in stream bed in the downstream.

CONCLUSIONS

From this research paper, it could be concluded that the numerical solution for the problem of the channel junction with the combining flow was approximately consistent with the field investigation presented in this research paper. Also, the study showed that both the junction angle and the discharge ratio had an effective influence on the free streamline coordinates. The studying of the bed profile showed that a sedimentation zone was occurred downstream the outlets accompanied with the flow separation zone. Also, the deposition occurs upstream the distributing junction due to the effect of the transverse flow towards the intakes, which result in a bigger average fall velocity of the suspended sediment than the average longitudinal flow velocity at that zone. The analysis of the field data showed that the maximum flow depth is directly proportional to the maximum sedimentation width. Also, the relatively smooth slope angle of the combining channel decreases the effect of the tributary flow on the scour in main channel.

NOMENCLATURE

a constants;
b constants;
b_1 width of first channel at the junction;
b_2 width of second channel at the junction;
b_3 width of third channel at the junction;
C_f constant;
d grain diameter= d_{50} for nonuniform bed material;
D_s particle diameter;
F constant = 0.79;
K_1 constant;
R hydraulic radius;
S longitudinal slope of water surface;
V_1 mean velocity at branches 1;
V_2 mean velocity at branches 2;
V_x velocity component in X direction;
V_y velocity component in Y direction;
W fall velocity m/sec;
α junction angle;
ω complex variable representing rectangular flow field = $\varphi + i\psi$;
τ_b shear stress on bed;
γ specific weight of the flow;
ρ_s sediment density;
ρ fluid density;
ν kinematic viscosity (10^{-6} m^2/s);
γ specific weight of water;
γ_s specific weight of bed particles; and
f, φ, and ξ are auxiliary variables.

Acknowledgements

The measured field data in this paper were carried out in co-operation with Hydraulic Research Institute (HRI), the National Water Research Centre, Ministry of Water Resources and Irrigation. The different instruments, the apparatuses, and the financial support of this investigation which were provided from the Hydraulic Research Institute (HRI) are gratefully acknowledged.

REFERENCES

1- Best, J. L., and Reid, I., "Separation zone at open channel junctions" J. Hydr. Engrg., ASCE, 110 (11), 1588-1594, 1984.
2- Biron, P., Best, J. L., and Roy, A. G., "Effects of bed discordance on flow dynamics at open-channel confluences" J. Hydr. Engrg., ASCE, 122 (121), 676-682, 1996.
3- Hydraulic Research Institute (HRI), "Hydraulic model design of Talkha power plant", Technical report, Delta barrages, Egypt, 2003.
4- Hsu, C. C., Lee, W. J., and Chang, Chang, C. H., "Subcritical open-channel junction flow" J. Hydr. Engrg., ASCE, 124 (8), 847-847, 1998b.
5- Joy, D. M., and Townsend, R. D., "Improved flow characteristics at a 90° channel confluences" 5th Con. Hydrotechnical Conf. Canadian Society for Civil Engineering, National Research Council Press, Ottawa, 781-799.
6- Kalinske, A.A., "Criteria for determining sand transport by surface creep and saltation" Trans. Am. Geophys. Union, Vol. (23), 1942.
7- Larry, J. Weber, Eric D. Schumate, and Nicola, "Experiments on flow at A 90° open-channel junction" J. Hydr. Engrg., ASCE, Vol. 127, No 5, May 2001.
8- Lin, J. D., and Soong, H. K., "Junction losses in open-channel flows" Water Resources Res., 15(2), 414-418, 1979.
9- Pashupati N. Modi, Pitamber D. Ariel and Mohan M. Dandekar, "Conformal mapping for channel junction flow" J. Hydr. Engrg., ASCE, Vol. 107, No HY12, December 2001.
10- Ramamurthy, A. S., Carballada, L. B., and Tran, D. M., "Combining open-channel flow at right angled junctions" J. Hydr. Engrg., ASCE, 114 (12), 1449-1460, 1988.
11- Ruby, W. W., "Settling velocities of gravel, sand and silt", A. J. of Science, Vol. 25, pp. 325-338., 1933.
12- Shazy Shabayek, Peter Steffler, and Faye Hicks, "Dynamic model for subcritical combining flow in channel junctions" J. Hydr. Engrg., ASCE, Vol. 128, No. 9, September 1, 2002.
13- Taylor, E. H., "Flow characteristics at rectangular open-channel junctions" Trans. ASCE, 109, 893-902, 1944.
14- Webber, N. B., and Greated, C. A., "An investigation of flow behavior at the junction of rectangular channel" Proc., Inst. of Civil. Engrs, Vol. 34, Thomas Telford Ltd., London, 321-334, 1966.

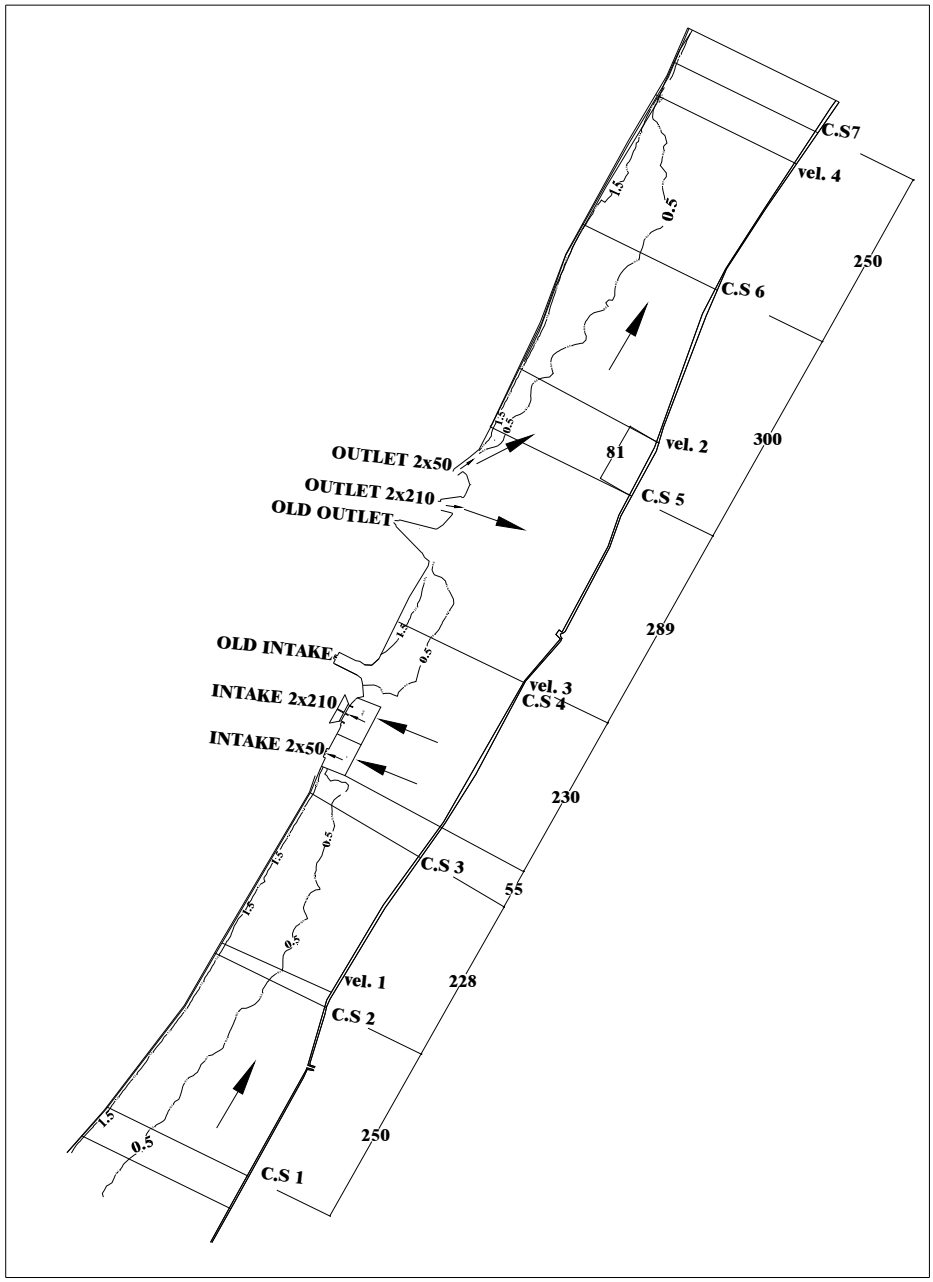

Fig. 2 General layout of Talkha Power Plant on Damietta Nile branch.

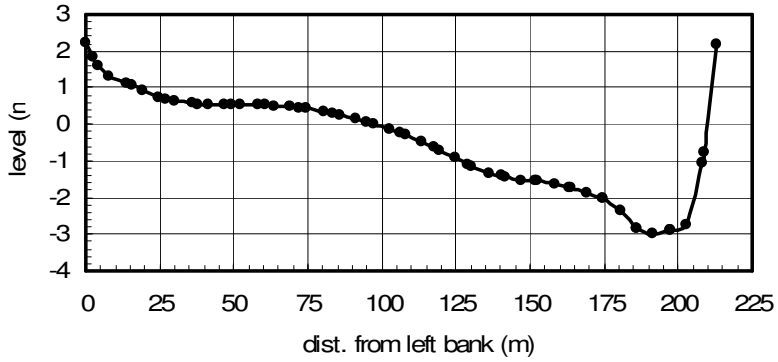

Fig. 3-a Cross-section No. 1 at km 143.667

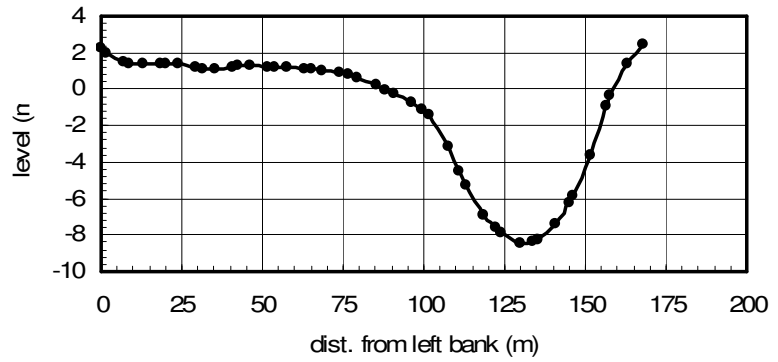

Fig. 3-b Cross-section No. 2 at km 143.917

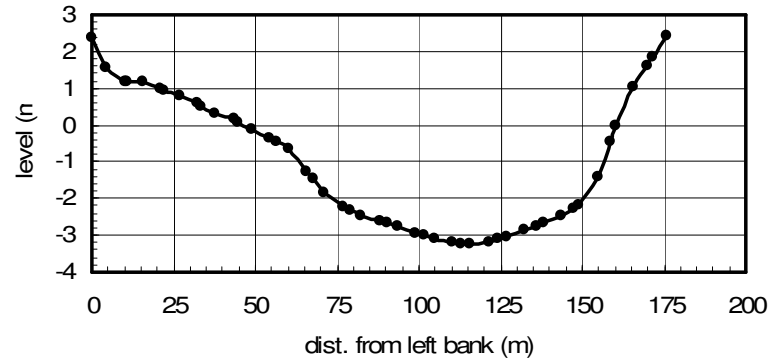

Fig. 3-C Cross-section No. 3 at km 144.145

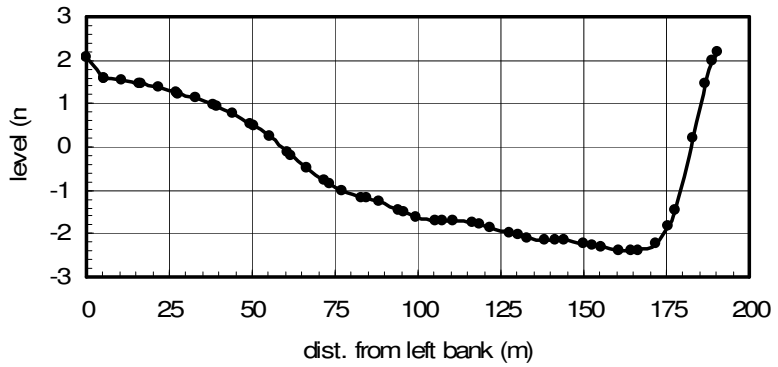

Fig. 3-D Cross-section No. 4 at km 144.430

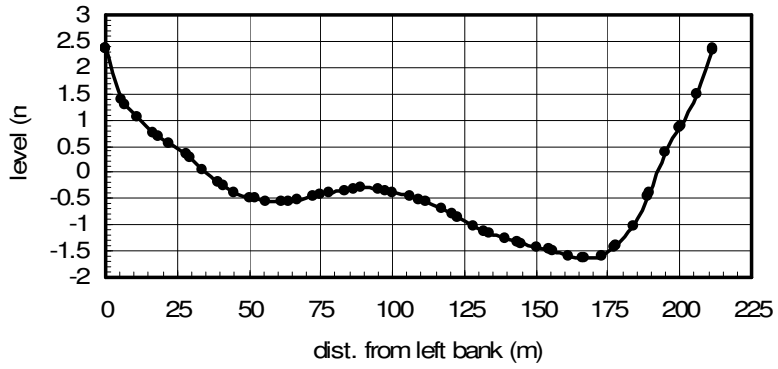

Fig. 3-E Cross-section No. 5 at km 144.719

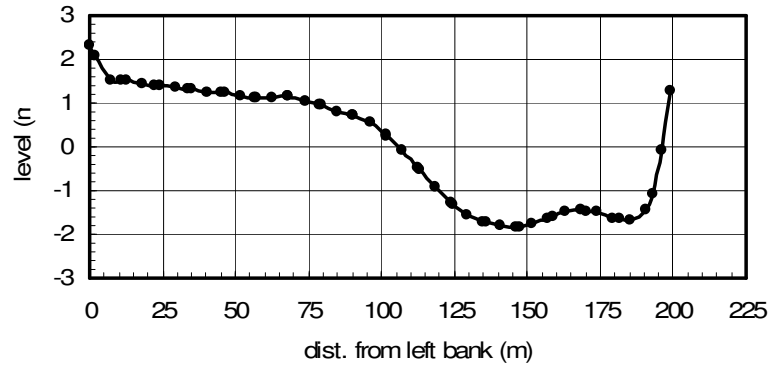

Fig. 3- F Cross-section No. 6 at km 145.019

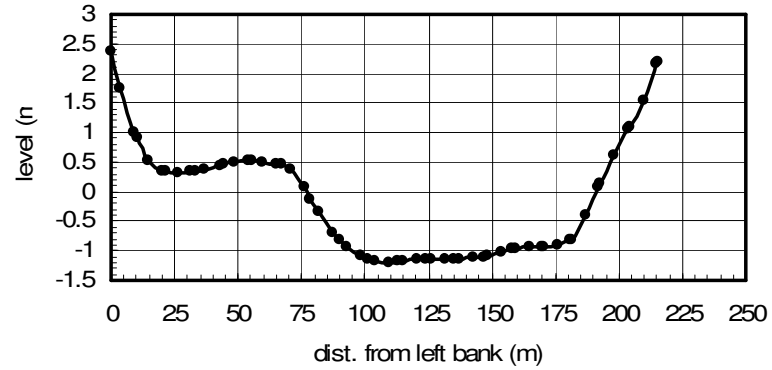

Fig. 3-G Cross-section No. 7 at km145.269

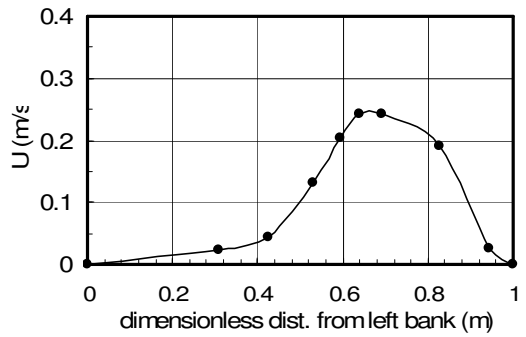

Fig. 4-A The velocity distribution along the transverse cross-section No.2.

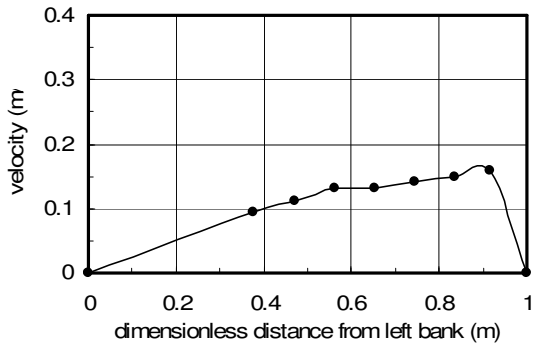

Fig. 4-B The velocity distribution along the transverse cross-section No.4.

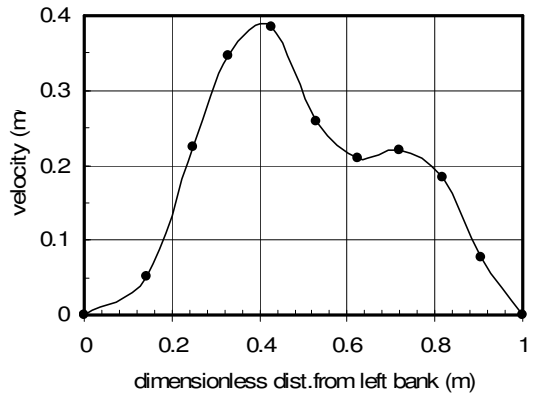

Fig. 4-C The velocity distribution along the transverse cross-section at 8.01 m from cross-section No.5.

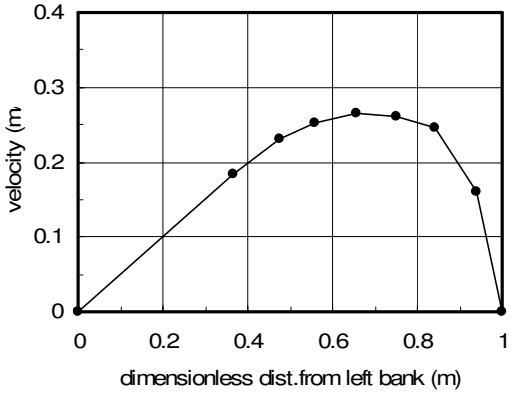

Fig. 4-d The velocity distribution along the transverse cross-section at 50.0 m from cross-section No.7.

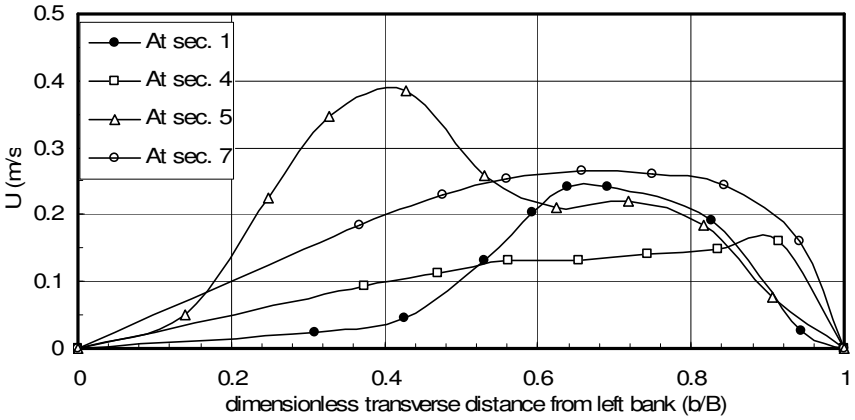

Fig. 4-E Comparison among velocity distributions at different cross-sections.

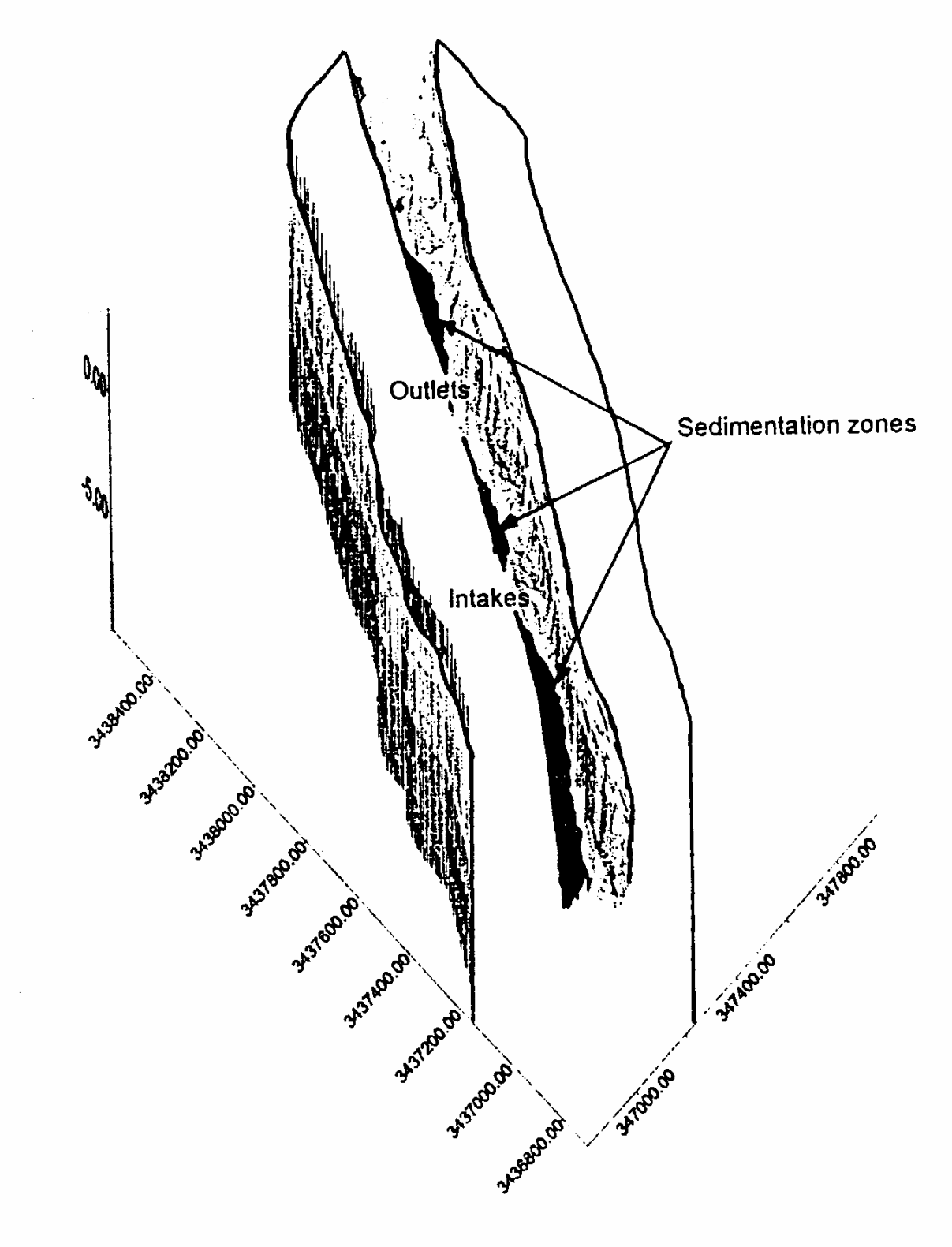

Fig. 5 Isometric view of the stream at both the intakes and the outlets of Talkha thermal power plant

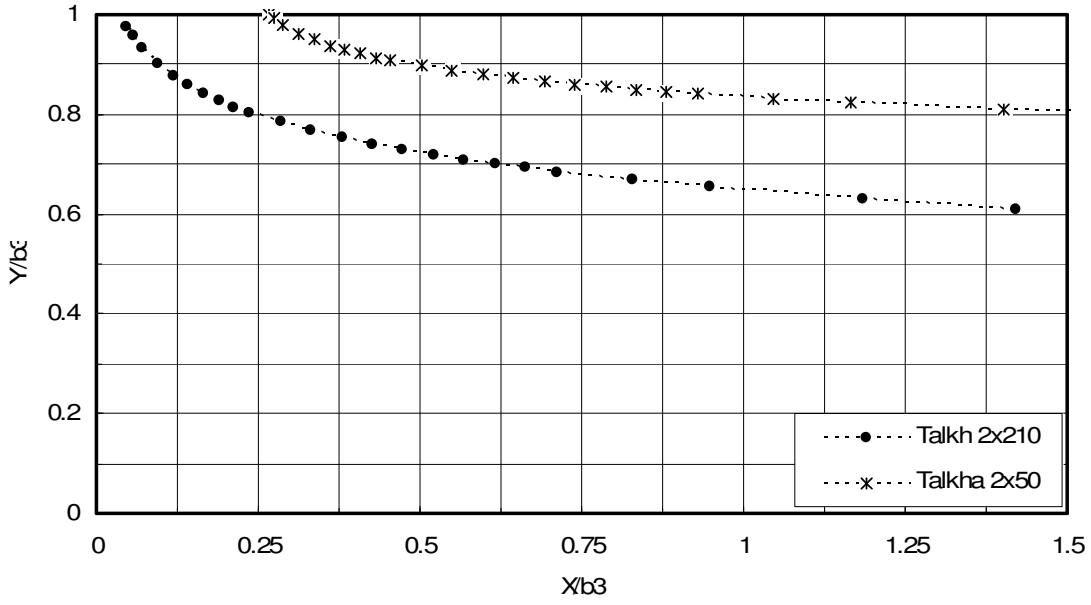

Fig. [6] predicted free streamlines for two outlets of Talkha power station

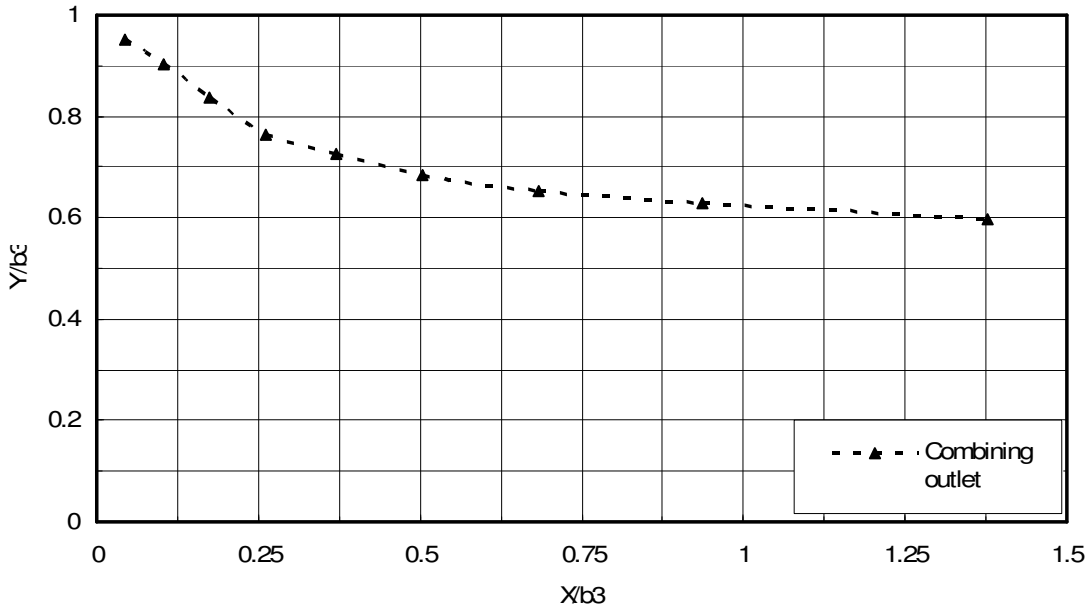

Fig. [7] predicted free streamline of combining outlet of Talkha thermal power plant.

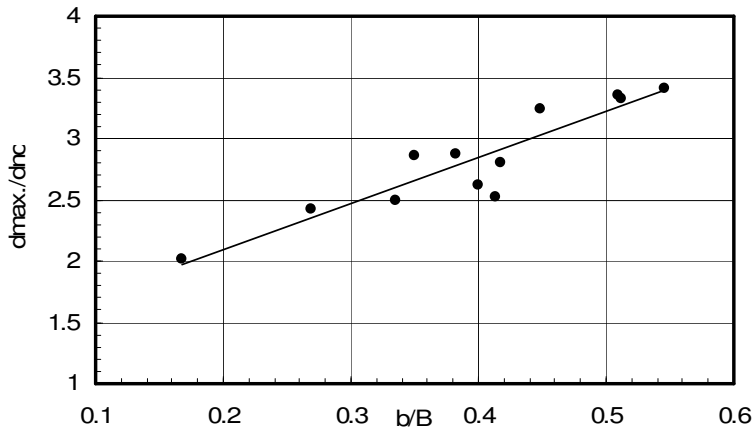

Fig. (8) The relationship between the maximum flow depth versus the sedimentation width at different cross-sections U.S. the intake

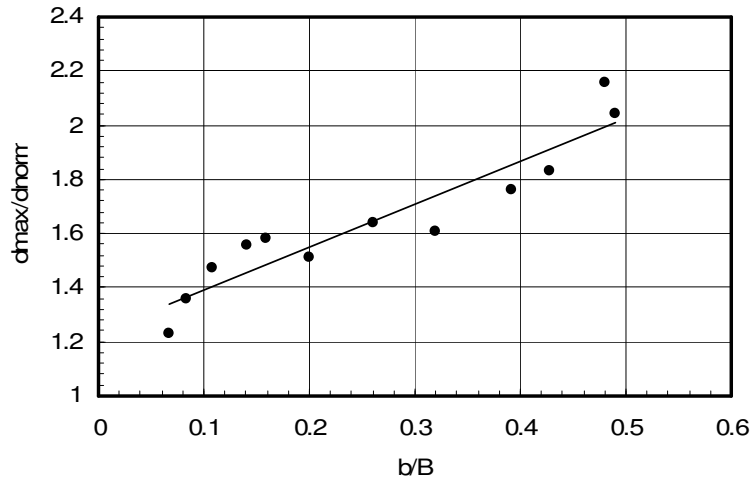

Fig. 9 The relationship between the maximum flow depth versus the sedimentation width at different cross-sections D.S. the outlet

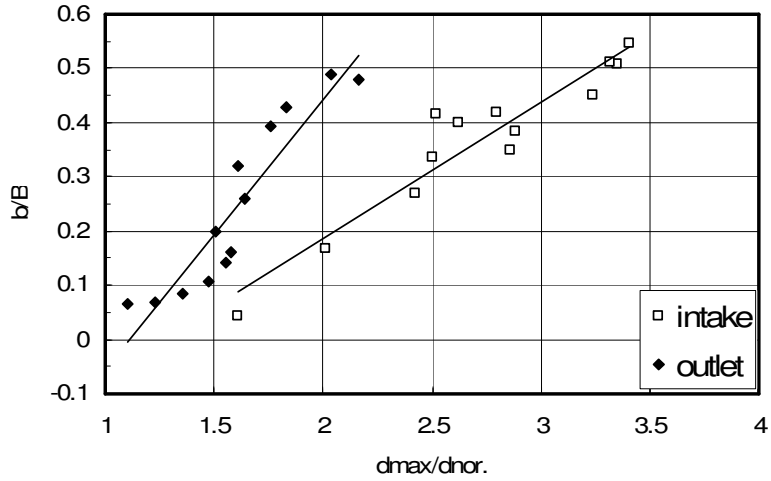

Fig. 10 A comparison between the sedimentation width and the maximum flow depth at the intake and the outlet.